https://doi.org/10.3311/PPch.13172

Periodica Polytechnica Chemical Engineering, 64(1), pp. 135–145, 2020

CFD Analysis of CO_2 Sequestration Applying Different Absorbents Inside the Microporous PVDF Hollow Fiber Membrane Contactor

Ali Taghvaie Nakhjiri[1], Amir Heydarinasab[1*]

[1] Department of Chemical Engineering, Science and Research Branch, Islamic Azad University, Simon Bulivar Blvd, Tehran, 1477893855, Iran
[*] Corresponding author, e-mail: a.heidarinasab@srbiau.ac.ir

Received: 20 September 2018, Accepted: 28 November 2018, Published online: 22 January 2019

Abstract

The sequestration process of greenhouse contaminants such as CO_2 via hollow fiber membrane contactor (HFMC) is regarded as a promising technology to manage the deleterious impressions of CO_2 on environment such as global warming and air pollution. This investigational paper renders a wide-ranging 2D simulation in order to assess the removal performance of CO_2 from CO_2/CH_4 gaseous stream (containing 80 % CH_4 and 20 % CO_2) in the HFMC. As the novelty, the evaluation of CO_2 acid gas removal from gaseous mixture applying four novel absorbing agents (potassium threonate (PT), piperazine (PZ), pure water (H_2O) and methyldiethanolamine (MDEA)) is implemented in the HFMC with the aim of introducing a more efficient liquid absorbent for CO_2 sequestration. Model validation is done based on the comparison of mathematical model outcomes and experimental data in a wide range of H_2O velocity and confirms a desirable agreement with an average relative deviation (ARD) of approximately 3 % for CO_2 flux. It is perceived from the results that PZ is introduced as the most efficient liquid absorbent for CO_2 sequestration and MDEA, PT and H_2O are in the next category (100 % removal using PZ > 96 % removal using MDEA > 89 % removal using PT > 57 % removal using H_2O). The results corroborate that increase in membrane tortuosity and gas velocity negatively affects the sequestration process while increment of module length and porosity improve the separation of CO_2.

Keywords

absorbent, CO_2 sequestration, membrane contactor, modeling and simulation, CO_2/CH_4 gaseous stream

1 Introduction

Nowadays, increase in the emission of greenhouse contaminants has eventuated in serious climate change and caused worldwide concern in environmental, scientific and political fields. Therefore, major impurities of industrial gaseous flows such as CO_2 and H_2S are required to be removed efficiently with the aim of mitigating the deleterious influences of them on environment and industry such acid rain, global warming and the corrosion of pipelines [1-3]. Different techniques such as cryogenic distillation, absorption and currently membrane separation process have been emerged in order to eliminate carbon dioxide from gaseous streams [4-6]. Gas-liquid membrane contactor is a novel technology that has been able to solve the serious disadvantages of conventional absorbers / disrobers affect on the removal efficiency of membrane contactor as like as foaming, unloading and also channeling [7].

Apart from decreasing the abovementioned disadvantages, the hollow fiber membrane contactor (HFMC) is modular and easy to scale up which eventuates in higher proportion of surface area to volume [7]. Despite various advantages, membrane may decline the performance of the hollow fiber membrane contactor by increasing the overall resistance [8]. The investigation on CO_2 separation from gaseous mixtures using hollow fiber membrane contactor has been conducted since 1980. Qi and Cussler [9] were the first investigators who developed the first membrane with the aim of removing carbon dioxide acid gas from gas stream. Liquid absorbent plays an essential role for carbon dioxide elimination in the HFMCs. Based on the physicochemical properties of absorbent solvents as like as thermal stability, reaction rate with CO_2 and the ease of regeneration, various alkanolamine solutions such

Cite this article as: Nakhjiri, A. T., Heydarinasab, A. "CFD Analysis of CO_2 Sequestration Applying Different Absorbents Inside the Microporous PVDF Hollow Fiber Membrane Contactor", Periodica Poolytechnica Chemical Engineering, 64(1), pp. 135–145, 2020. https://doi.org/10.3311/PPch.13172

as diethanolamine (DEA), monoethanolamine (MEA), diisopropanolamine (DIPA) and triethanolamine (TEA) were applied as liquid absorbents for the separation of CO_2 acid gas from gaseous stream [10-15].

Generally, there are two prevalent liquid absorbents for selective separation of CO_2, SO_2 and H_2S acid pollutants from gaseous flows: physical and chemical liquid solvents [16-18]. Alavinasab et al. [17] used both distilled water as a physical absorbing agent and 2-amino-2 methyl-1-propanol (AMP) as a chemical liquid solvent with the aim of comparing the difference between physical absorption and chemical absorption of CO_2. They discovered that in the counter-current flow arrangement, the utilization of AMP increased the sequestration efficiency of CO_2 by about 16 % compared to distilled water [17]. The sequestration behavior of CO_2 applying three conventional alkanolamines such as diethanolamine (DEA), 2-amino-2 methyl-1-propanol (AMP) and diisopropanolamine (DIPA) through hollow fiber membrane contactor was presented by Boucif et al. [19]. They corroborated that AMP could sequester CO_2 acidic contaminant from gaseous mixture better than DEA and DIPA [19]. Atchariyawut et al. [16] investigated the influence of temperature and velocity of liquid absorbent on CO_2 flux along with the mass transfer analysis of sequestration process. Hot potassium carbonate (K_2CO_3) and liquid absorbent was applied by Mehdipour et al. [20] to evaluate the separation efficiency of CO_2 from gaseous mixtures via a microporous HFMC. They understood that increment in the velocity of gaseous flow from 0.1 to 0.3 m s^{-1} significantly enhanced the CO_2 absorption flux from 6.25×10^{-4} to 7.75×10^{-4} mol m^{-2} s^{-1} [20]. The influence of potassium glycinate (PG), sodium hydroxide (NaOH) and potassium argininate (PA) absorbents on the sequestration performance of CO_2 was studied by Nakhjiri et al. [21]. They perceived that PA could sequester about 95 % of inlet CO_2 while the sequestration efficiency of CO_2 using PG and NaOH was only 62 and 57 % of CO_2, respectively [21].

Currently, different investigators developed the finite element method (FEM) with the aim of evaluating the sequestration percentage of greenhouse pollutants such as CO_2 and H_2S from various gaseous mixtures [12, 13, 22-25]. Besides, numerous researchers applied COMSOL software, which is based on FEM to implement the computational fluid dynamics (CFD) simulation of CO_2 separation from gaseous mixtures [12, 13, 20, 26]. They reported reasonable precision compared to experimental data. Considering the abovementioned items, COMSOL is applied in this article to provide CFD analysis of CO_2 sequestration from CO_2 / CH_4 gaseous stream under non-wetting mode of operation.

In this investigational paper, a wide-ranging 2D simulation is presented with the goal of studying the CO_2 sequestration efficiency from gaseous stream containing 20 % CO_2 and 80 % CH_4. Numerical simulation is implemented under non-wetting mode of operation and counter-current pattern of gas and liquid. As the novelty, physical solvent (H_2O) and chemical solvents (potassium threonate (PT), piperazine (PZ) and methyldiethanolamine (MDEA)) are utilized for CO_2 separation. Various parameters which affect the sequestration efficiency of CO_2 via HFMC such as gas velocities, porosity and tortuosity of hollow fiber membrane contactor and module length are under the investigation.

2 Mass Transfer in Microporous HFMC

The transport of interested gas (CO_2) from the gas phase through the microporous PVDF membrane into liquid phase is vividly demonstrated by Fig. 1 and can be explained by the resistance-in-series model, presented by Eq. (1) [27]:

$$\frac{1}{K_{Ol}} = \frac{1}{k_l} + \frac{Hd_0}{k_m d_{\ln}} + \frac{Hd_0}{k_g d_i}. \tag{1}$$

Where in this equation, K_{Ol} is expressed as the overall mass transfer coefficient in the liquid phase. k_g, k_m and k_l are the local mass transfer coefficients in the gas phase, membrane phase and liquid phase, respectively. H, d_0, d_i and d_{ln} are respectively denoted as Henry's constant, the outer, inner and logarithmic average diameters of the fibers. Eq. (2) presents the Yang and Cussler [28] mass transfer correlation with the aim of predicting the CO_2 transfer coefficient inside the shell compartment:

$$Sh = \frac{k_{CO_2,g} d_i}{D_{CO_2,g}} = 1.25\left(\frac{d_e}{L}\mathrm{Re}\right)^{0.93} Sc^{0.33}. \tag{2}$$

In this equation, d_e is denoted as the hydraulic diameter of shell. The CO_2 mass transfer coefficient in the membrane side ($k_{CO_2,gm}$) is derived by Eq. (3):

$$k_{CO_2,gm} = \frac{D_{CO_2,g} \times \varepsilon}{\tau\delta}. \tag{3}$$

Where ε, τ and δ are membrane's porosity, tortuosity and thickness, respectively. Equation (4) renders the reputable Graetz-Leveque mass transfer correlation for accurate estimation of liquid mass transfer in the tube compartment (k_l) [29]:

$$Sh = \frac{k_l d_i}{D_{CO_2,liq}} = 1.62\left(\frac{d_i}{L} Re.Sc\right)^{\frac{1}{3}}. \tag{4}$$

Where Sh, Re and Sc are respectively expressed as the Sherwood number, Reynolds number and Schmidt number.

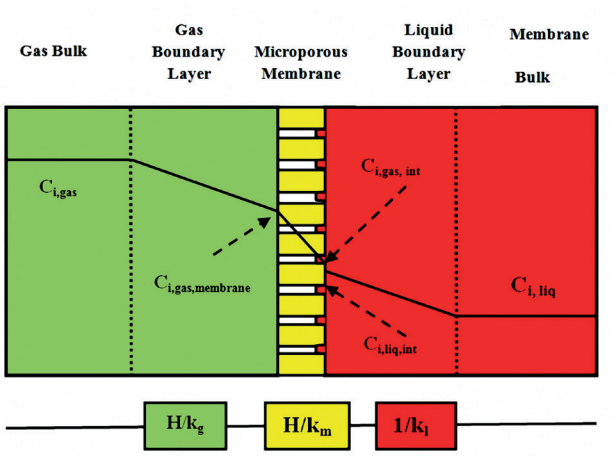

Fig. 1 Mass transfer areas and resistance-in-series in all domains of HFMC considering non-wetting mode of operation.

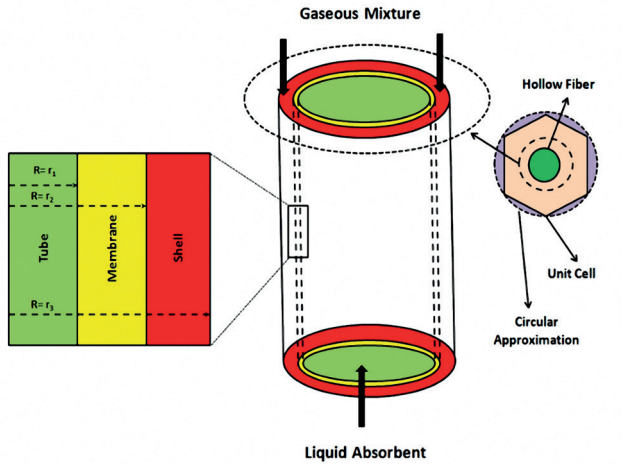

Fig. 2 Schematic diagram and circular approximation of the porous PVDF hollow fiber membrane contactor (HFMC).

3 Theory of Model

The major purpose of this article is to represent a comprehensive dynamic modeling and a wide-ranging 2D numerical simulation of CO_2 separation from gaseous flow via hollow fiber membrane contactor utilizing PT, PZ, H_2O and MDEA absorbents. Continuity equations are derived and consequently solved in three main domains including tube side (liquid phase), porous membrane side and shell section (gas phase). The diagrammatic scheme and circular approximation of the porous PVDF hollow fiber membrane contactor is apparently demonstrated in Fig. 2. Based on the Happel's [30] free surface model, the fiber's cross sectional region is assumed to be circle-shaped which is clearly demonstrated in Fig. 2. It is obvious from the schematic diagram that the gaseous stream is fed into the shell segment of the HFMC, passes through the pores of membrane and eventually is absorbed by PT, PZ, H_2O and MDEA stripping absorbents. Due to the assumption of non-wetting mode of operation, only the diffusion of gas phase occurs in the membrane side of the hollow fiber membrane contactor and liquid absorbents flow in the tube side of HFMC based on counter-current form.

Module specification, operating conditions and also physicochemical properties of CO_2 acid gas and PT, PZ, H_2O and MDEA absorbents utilized in modeling and numerical simulation are illustrated in Table 1 and Table 3, respectively. Following assumptions are implemented to develop the dynamic modeling and numerical simulation:

1. Steady state and isothermal conditions,
2. Non wetting mode of operation,
3. The utilization of Henry's law for the interface of gas and liquid,
4. The application of Happel's free surface model with the purpose of anticipating the species velocity profile in the liquid phase (tube section),
5. The existence of ideal gas behavior in the tube segment of hollow fiber membrane contactor,
6. The consideration of laminar liquid flow in the tube side and laminar gas flow in the shell side,
7. The existence of a fully developed laminar parabolic gas velocity profile in the shell side of the hollow fiber membrane contactor and
8. Counter-current arrangement of liquid-gas flow.

Fig. 3 shows the molecular structures of PT, PZ, H_2O and MDEA used as absorbing agents in this investigation.

Table 1 Hollow fiber membrane contactor parameters and operating conditions applied for numerical analysis [16, 31].

Parameter	Value	Unit
Type of membrane	PVDF	--
Inner fiber radius (r_1)	3.25×10^{-4}	m
Outer fiber radius (r_2)	5×10^{-4}	m
Module inner radius (R)	5×10^{-3}	m
Effective contact area	0.019	m^2
Module length	0.27	m
ε (Porosity)	0.75	--
τ (Tortuosity)	$(2-\varepsilon)^2/\varepsilon$	--
Number of fibers	50	--
Temperature (T)	303.15	K
Gas velocity (V_g)	0.07	m s^{-1}
Liquid velocity (V_l)	2.3	m s^{-1}
P	1	atm

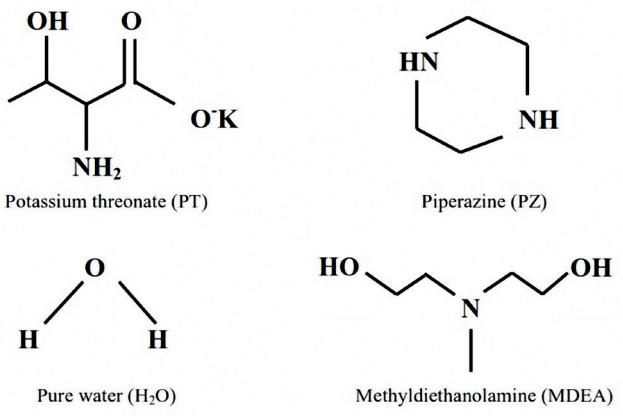

Fig. 3 Molecular structures of chemical liquid solvents used in this investigation.

3.1 Governing Equations in the Tube Region

The steady state material balance for species *i* (CO_2, PT, PZ, H_2O and MDEA liquid absorbents) in the tube side of HFMC considering principal mechanisms (diffusion, convection and also reaction) may be derived as Eq. (5) [13]:

$$D_{i-tube}\left[\frac{\partial^2 C_{i-tube}}{\partial r^2}+\frac{1}{r}\frac{\partial C_{i-tube}}{\partial r}+\frac{\partial^2 C_{i-tube}}{\partial z^2}\right] = V_{z-tube}\frac{\partial C_{i-tube}}{\partial z}-R_i. \quad (5)$$

It can be denoted from the equation that D_{i-tube} is diffusion coefficient of components *i* (CO_2, PT, PZ, H_2O and MDEA) inside the tube region of HFMC and also R_i and V_{z-tube} are described as the reaction rate and the velocity in the axial direction, respectively. On the basis of Newtonian laminar flow, the estimation of axial velocity distribution is as Eq. (6) [13]:

$$V_{z-tube}=2\overline{V_t}\left[1-\left(\frac{r}{r_1}\right)^2\right]. \quad (6)$$

In Eq. (6) $\overline{V_t}$, r and r_1 express the average velocity inside the tube section, radial coordinate and the radius of inner fiber, respectively. Table 2 lists the reaction of CO_2 with physical absorbent (H_2O) and chemical absorbents (PT, PZ, H_2O and MDEA) involved in CO_2 sequestration.

The reaction rates of CO_2 acid pollutant with PT, PZ, H_2O and MDEA absorbent solutions inside the tube compartment of hollow fiber membrane contactor are rendered by Eqs. (7) to (10), respectively [34-37].

$$r_{CO_2-PZ}=-4.4910^{12}\ \exp(-5712/T)C_{CO_2}C_{PZ} \quad (7)$$

$$r_{CO_2-PT}=-4.1310^{8}\ \exp(-3580/T)C_{PT}\ \exp(0.9C_{PT})C_{CO_2} \quad (8)$$

$$r_{CO_2-H_2O}=-1.210^{4}\ C_{OH^-}C_{CO_2} \quad (9)$$

$$r_{CO_2-MDEA}=-8.7411012^{12}\ \exp(-8625/T)C_{CO_2}C_{MDEA}. \quad (10)$$

Table 2 Reaction of CO_2 with physical and chemical absorbents

Absorbent	Reaction	Ref
PT	$CO_2+2RNH_2\rightarrow RNHCOO^-+RNH_3^+$	[32]
PZ	$PZ+CO_2+H_2O\rightarrow HCO_3^++PZCOO^-$	[33]
H_2O	$H_2O+CO_2\leftrightarrow H^++HCO_3^-$ $OH^-+CO_2\leftrightarrow HCO_3^-$	[34]
MDEA	$R_1R_2R_3N+H_2O+CO_2\rightarrow R_1R_2R_3NH^++HCO_3^-$	[35]

Table 3 CO_2, PT, PZ, H_2O and MDEA physicochemical properties used for dynamic modeling and simulation.

Parameter	Value	Unit	Ref
$D_{CO_2-Shell}$	1.8×10^{-5}	$m^2\ s^{-1}$	[13]
D_{CO_2-mem}	$D_{CO_2-Shell}(\varepsilon/\tau)$	$m^2\ s^{-1}$	[13]
D_{CO_2-PT}	1.38×10^{-9}	$m^2\ s^{-1}$	[38]
$D_{CO_2-H_2O}$	$2.35\times10^{-6}\exp(-2199/T)$	$m^2\ s^{-1}$	[39]
D_{CO_2-PZ}	1.51×10^{-9}	$m^2\ s^{-1}$	[34]
D_{CO_2-MDEA}	1.18×10^{-9}	$m^2\ s^{-1}$	[40]
$D_{PT-tube}$	8.45×10^{-10}	$m^2\ s^{-1}$	[41]
$D_{PZ-tube}$	1.05×10^{-9}	$m^2\ s^{-1}$	[34]
$D_{H_2O-tube}$	$1.18\times10^{-6}\exp(-2199/T)$	$m^2\ s^{-1}$	[39]
$D_{MDEA-tube}$	6.21×10^{-10}	$m^2\ s^{-1}$	[40]
m_{CO_2-PT}	1.5		[37]
m_{CO_2-PZ}	1.06		[37]
$m_{CO_2-H_2O}$	0.83		[37]
m_{CO_2-MDEA}	0.82		[37]
OH^- concentration	$K_W/K_p((1-m_{PA})/m_{PA})$	mol m^{-3}	[42, 43]

3.2 Governing Equations in the Membrane Region

In the membrane side of HFMC, non-wetting mode of operation is assumed. Therefore, the only mechanism which may be considered for CO_2 transport inside the microporous PVDF membrane is diffusion. The governing material balance in the steady state mode can be presented as Eq. (11) [13]:

$$D_{CO_2-mem}\left[\frac{\partial^2 C_{CO_2-mem}}{\partial r^2}+\frac{1}{r}\frac{\partial C_{CO_2-mem}}{\partial r}+\frac{\partial^2 C_{CO_2-mem}}{\partial z^2}\right]=0. \tag{11}$$

C_{CO_2-mem} and D_{CO_2-mem} in this equation indicate the concentration and diffusion coefficient of CO_2 across the microporous polyvinylidene fluoride (PVDF) membrane. The diffusion coefficient of carbon dioxide in the microporous PVDF membrane depends on two variables: 1) membrane porosity (ε) and 2) membrane tortuosity (τ) and may be defined as Eq. (12) [13]:

$$D_{CO_2-mem}=\left[\frac{D_{CO_2-shell}\times\varepsilon}{\tau}\right]. \tag{12}$$

3.3 Governing Equations in the Shell Region

The governing differential mass transfer balance under the steady state mode of operation in order to transport of CO_2 inside the shell is given as Eq. (13) [13]:

$$D_{CO_2-shell}\left[\frac{\partial^2 C_{CO_2-shell}}{\partial r^2}+\frac{1}{r}\frac{\partial C_{CO_2-shell}}{\partial r}+\frac{\partial^2 C_{CO_2-shell}}{\partial z^2}\right] = V_{z-shell}\frac{\partial C_{CO_2-shell}}{\partial z}. \tag{13}$$

Based on the assumption of Happel's free surface model, the profile of velocity inside the shell region of HFMC is presented as Eq. (14) [13]:

$$V_{z-shell}=2\overline{V_s}\left[1-\left(\frac{r_2}{r_3}\right)^2\right]\times\left[\frac{\left(r/r_3\right)^2-\left(r_2/r_3\right)^2+2\ln\left(r_2/r\right)}{3+\left(r_2/r_3\right)^4-4\left(r_2/r_3\right)^2+4\ln\left(r_2/r_3\right)}\right]. \tag{14}$$

In Eq. (14) $\overline{V_s}$ is average velocity inside the shell region of HFMC. Also r_3 is the shell's effective radius and may be presented as Eq. (15) [13]:

$$r_3=r_2\sqrt{1/\left(1-\varphi\right)}. \tag{15}$$

φ is the void's volume fraction and can be calculatted by Eq. (16):

$$1-\varphi=\frac{nr_2^2}{R^2}. \tag{16}$$

In which, R^2 and n are defined as the inner radius of module and number of fibers, respectively. Therefore, using Eqs. (10) and (11), the effective radius of shell based on happel's free surface model is achieved 8.45×10^{-4} m.

Boundary conditions utilized inside the tube, porous membrane and shell regions of hollow fiber membrane contactor are listed in Table 4.

3.4 Numerical Scheme

The prominent purpose of this research article is to present a dynamic modeling and a wide-ranging 2D comprehensive simulation for CO_2 capture from CO_2/CH_4 gaseous stream applying novel liquid stripping absorbents (PT, PZ, H_2O and MDEA) in microporous HFMC using CFD technique. According to this reason, COMSOL Multiphysics software which is based on finite element method (FEM) was utilized to solve the governing equations in the tube, membrane and shell sides of HFMC. Due to undeniable and various abilities such as memory efficiency, robustness and the simplicity to use for solving widespread symmetric linear systems, PARDISO numerical solver was used to control the material balance error. In order to solve partial differential equations, a computational platform consisting of 64-bit operating system, Intel core™ i5-4200U CPU at 1.60 GHz and 4 Gigabyte RAM was used. The computational duration for solving the equations of the model was approximately 3 minutes. Fig. 4 and Fig. 5 demonstrate the triangular mesh elements employed to analyze gaseous mixture behavior inside the microporous HFMC and convergence status of 2D simulation, respectively. It is apparent from the Fig. 4 that due to the existence of reaction and gas-liquid contact inside the pores of membrane

Table 4 Boundary conditions utilized for model development

Boundary	Tube side	Membrane side	Shell side
$z=0$	$C_{CO_2-tube}=0$ $C_{solvent-tube}=C_{initial}$	Insulated	$\frac{\partial C_{CO_2-shell}}{\partial r}=0$
$z=L$		Insulated	$C_{CO_2-shell}=C_{initial}$
$r=0$	$\frac{\partial C_{CO_2-tube}}{\partial r}=0$		
$r=r_1$	$C_{CO_2-tube}=m_{CO_2}C_{CO_2-mem}$	$C_{CO_2-mem}=\frac{C_{CO_2-tube}}{m_{CO_2}}$	
$r=r_2$		$C_{CO_2-mem}=C_{CO_2-shell}$	$C_{CO_2-shell}=C_{CO_2-mem}$

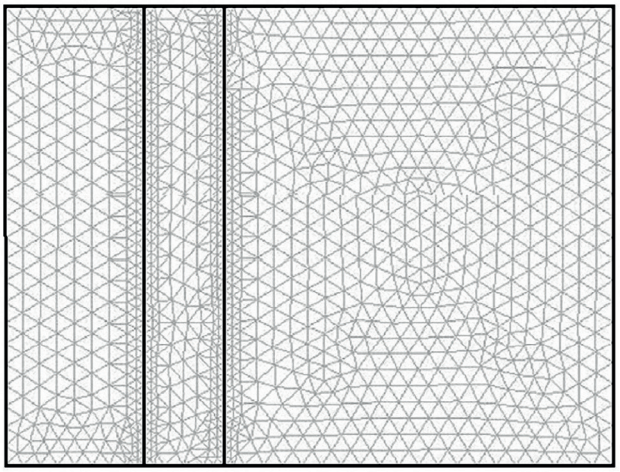

Fig. 4 Triangular meshing employed for the simulation.

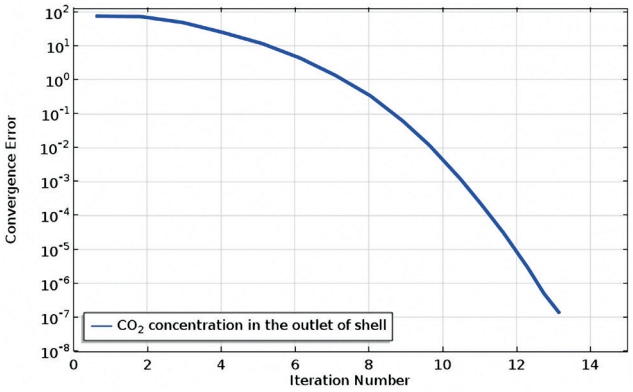

Fig. 5 Convergence status of numerical simulation.

compartment, the mesh size and density in this region is smaller than other areas to increase the outputs accuracy and reduce the computational discrepancies. Fig. 5 clearly illustrates that this system is non-stiff which provides confidence in the solution process and after 13 iterations the system reaches convergence.

It is worth mentioning that although increase in the number of meshes declines the computational errors, it dramatically increases the iterations and calculation time. Therefore, achieving the optimal number of meshes is mandatory. The influence of mesh numbers on the CO_2 concentration at the outlet of the microporous HFMC's shell compartment is illustrated in Fig. 6. It is understood from the Fig. 6 that increment in the mesh numbers leads in better convergence of simulation's results, but after the 260th mesh, no significant changes in CO_2 concentration at the shell side's outlet using different chemical absorbents occurs which implies the convergence of the simulation outcomes. Therefore, the computational precision is independent of the applied mesh numbers in values greater than 260.

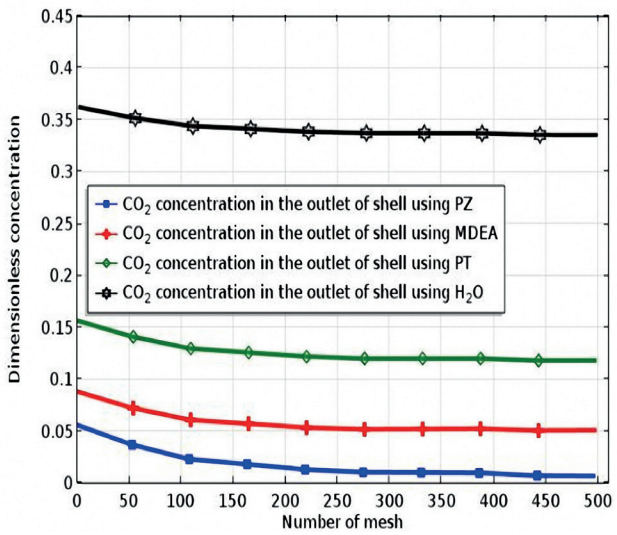

Fig. 6 Influence of mesh numbers on CO_2 concentration at the outlet of shell side using PT, PZ, H_2O and MDEA absorbents

4 Results and Discussion

4.1 Model Validation

Up to now, based on the knowledge of the authors, there is only one experimental article about the sequestration of CO_2 from CO_2/CH_4 gaseous stream using H_2O inside the microporous PVDF HFMC [16]. Hence the results of developed model are validated with the experimental data reported in the literature by Atchariyawut et al. [16]. Fig. 7 corroborates that there is an excellent agreement between the results of simulation and experimental data with an average absolute deviation (ARD) of about 3 % for CO_2 flux. The deviation between modeling results and experimental data are able to be justified due to the anticipation of reaction kinetics and constants.

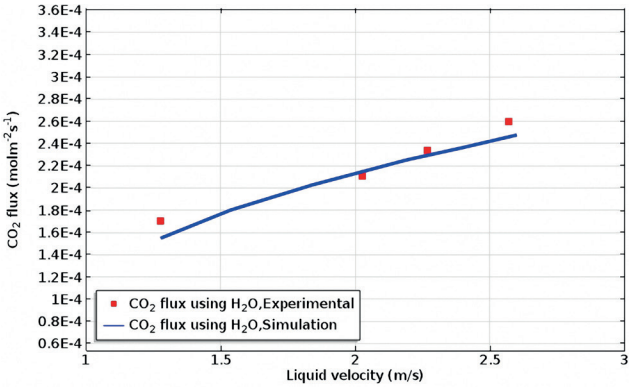

Fig. 7 Comparison of experimental data and simulation predictions for CO_2 flux in a wide range of liquid velocity in the microporous PVDF HFMC. *Feed gas* = 20/80 CO_2/CH_4, $C_{absorbents}$ = 1000 mol m^{-3}, Q_g = 200 ml min^{-1}, $T_{absorbent}$ = 303.15 K.

4.2 Concentration Distribution of CO_2

Fig. 8 demonstrates the dimensionless concentration distribution of CO_2 ($C_{CO_2}/C_{CO_{2,0}}$) inside the shell compartment of microporous hollow fiber membrane contactor using PT, PZ, H_2O and MDEA absorbing agents. Counter-current mode of operation justifies the movement of liquid absorbents inside the tube segment of HFMC where the concentration of CO_2 is zero (z = 0) and also the flow of CO_2/CH_4 gaseous stream in the other compartment (shell side) where the concentration of CO_2 is in the highest amount (maximum) ($z = L$). Overall, diffusion and convection can be regarded as two prominent mechanisms of gas transfer inside the HFMC. Diffusion mechanism happens in the radial direction (r) because of the gradient of concentration. Also, convection mechanism takes place in axial direction (z) due to the velocity of fluid. However, in the tube region of hollow fiber membrane contactor, diffusional mass transfer is preferred due to increasing CO_2 sequestration. The mechanism of CO_2 removal in the hollow fiber membrane contactor can be interpreted based on the transfer of gaseous stream into the pores of membrane to the other side and the absorption of CO_2 by moving absorbent agents (PT, PZ, H_2O and MDEA) inside the shell compartment.

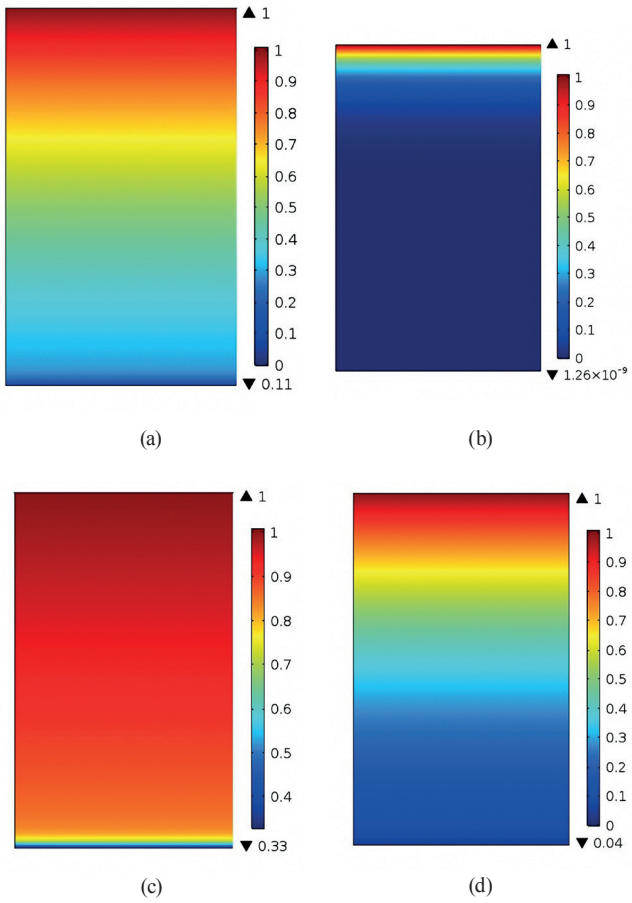

Fig. 8 Dimensionless concentration distribution of CO_2 inside the shell compartment of PVDF membrane contactor using (a) potassium threonate (PT), (b) piperazine (PZ), (c) pure water (H_2O) and (d) methyldiethanolamine (MDEA) liquid absorbents.
Feed gas = 20/80 CO_2/CH_4, r_1 = 0.325 mm, r_2 = 0.5 mm, r_3 = 0.845 mm, $C_{CO2,0}$ = 0.075 mol m^{-3}, $C_{absorbents}$ = 1000 mol m^{-3}, V_g = 0.07 m s^{-1}, V_l = 2.3 m s^{-1}, T = 303.15 K, P = 1 atm.

4.3 Axial Concentration Profile of CO_2 along the Shell-Membrane Interface

The axial concentration distribution of CO_2 along the shell-membrane interface of the HFMC utilizing PT, PZ, H_2O and MDEA liquid absorbents can be illustrated by Fig. 9. It is apparent from the Fig. 9 that at $z = L$, the concentration of CO_2 is maximum and decreased to the minimum amount at the outlet of shell side (z = 0). Also, it is understood from the Fig. 9 that the dimensionless concentration of CO_2 at the outlet of shell side (z = 0) using PZ absorbent is about 0 while the dimensionless concentration of CO_2 at the outlet of shell side using MDEA, PT and H_2O is 0.04, 0.11 and 0.33, respectively which indicate the excellent removal performance of CO_2 with PZ compared to MDEA, PT and H_2O (100 % removal using PZ > 96 % removal using MDEA > 89 % removal using PT > 57 % removal using H_2O).

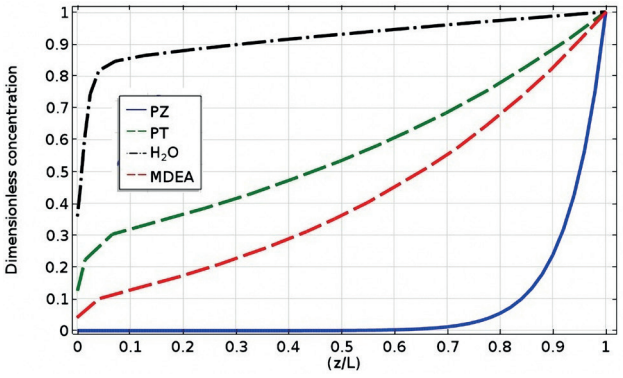

Fig. 9 Axial dimensionless concentration distribution of CO_2 along the shell-membrane interface using potassium threonate (PT), piperazine (PZ), pure water (H_2O) and methyldiethanolamine (MDEA) liquid absorbents.
Feed gas = 20/80 CO_2/CH_4, r_1 = 0.325 mm, r_2 = 0.5 mm, r_3 = 0.845 mm, $C_{CO2,0}$ = 0.075 mol m^{-3}, $C_{absorbents}$ = 1000 mol m^{-3}, V_g = 0.07 m s^{-1}, V_l = 2.3 m s^{-1}, T = 303.15 K, P = 1 atm.

4.4 The Effect of Membrane Porosity on CO_2 Removal

The influence of membrane porosity on CO_2 sequestration from CO_2/CH_4 gaseous stream using various absorbents (PT, PZ, H_2O and MDEA) is rendered by Fig. 10. The percentage of CO_2 removal is derived from Eq. (17) [44]:

$$\%\ CO_2\ removal = 100\left(\frac{C_{outlet}}{C_{inlet}}\right). \quad (17)$$

It is entirely apparent from the Fig. 10 that increment in the porosity of membrane from 0.1 to 0.9 eventuates in a significant increase in CO_2 removal from about 82 to approximately 100 % when PZ is used as the absorbent solution of process. However, using PT, H_2O and MDEA liquid solvents cause a reletively considerable increase in the sequestration percentage of CO_2 from almost 54 to 91 %, from 18 to 76 % and from 66 to 98 % while increasing the membrane porosity from 0.1 to 0.9. It means that a considerable removal of CO_2 from CO_2/CH_4 gaseous flow may be taken place by applying a microporous PVDF membrane with a porosity equal to 0.9 and PZ absorbent. Also it is clear that the efficiency of H_2O as absorbing agent for removing CO_2 from gaseous flow is considered insufficient. As it is clear from the Eq. (12) mentioned above, increment in the porosity of membrane increases the CO_2 diffusion coefficient inside the membrane segment of HFMC (D_{CO_2-mem}) and also improves the CO_2 mass transfer through the membrane. Consequently, whenever the membrane porosity increases, the transfer rate of CO_2 acidic gas inside the membrane wall improves significantly that leads to more superior CO_2 separation efficiency.

4.5 The Effect of Membrane Tortuosity on CO_2 Removal

Fig. 11 depicts the influence of membrane tortuosity on CO_2 removal using PT, PZ, H_2O and MDEA liquid absorbents. As can be seen in the abovementioned Eq. (11), the effective diffusion coefficient of CO_2 inside the membrane segment of HFMC (D_{CO_2-mem}) is in inverse relation with the membrane tortuosity. Hence, by increasing the tortuosity of membrane, a substantial increment in the mass transfer resistance of membrane takes place which results in a significant reduction in total mass transfer of CO_2. By decreasing total mass transfer resistance of the membrane, the diffusivity of CO_2 in the membrane declines which leads in the reduction of CO_2 absorption percentage. Increment in the tortuosity of membrane (from 1 to 5) leads in reducing the percentage of CO_2 removal from about 100 to 96 % using PZ, from about 92 to 82 % using PT, from about 90 to 82 % using MDEA and from 77.5 to 48 % using H_2O absorbent. Different decrements in CO_2 removal can be justified due to the difference of some constants and kinetics of reactions such as the reaction rates and the solubility of CO_2 in PS, PZ, MDA and H_2O liquid absorbents utilized for developing the computational simulation.

4.6 The Effect of Module Length on CO_2 Removal

Fig. 12 represents the influence of module length on the sequestration rate of CO_2 from CO_2/CH_4 gaseous stream in the microporous PVDF hollow fiber membrane contactor using four various absorbents (PT, PZ, H_2O and MDEA). As can be seen from the Fig. 12, by increasing the module length, residence time and also contact area between two phases (gas and liquid phases) through the HFMC increases substantially. Therefore, increase in the contact area and residence time inside the microporous HFMC provides better circumstances for efficient reaction of CO_2 molecules and liquid absorbents that positively encourages the CO_2 separation efficiency from gaseous stream. According to the

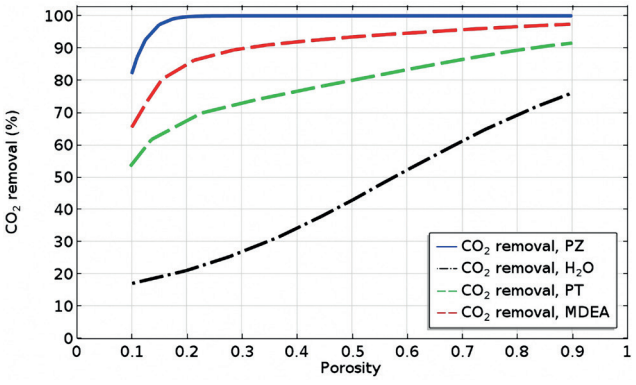

Fig. 10 The influence of membrane porosity on CO_2 removal using potassium threonate (PT), piperazine (PZ), pure water (H_2O) and methyldiethanolamine (MDEA) liquid absorbents.
Feed gas = 20/80 CO_2/CH_4, r_1 = 0.325 mm, r_2 = 0.5 mm, r_3 = 0.845 mm, $C_{CO2,0}$ = 0.075 mol m^{-3}, $C_{absorbents}$ = 1000 mol m^{-3}, V_g = 0.07 m s^{-1}, V_l = 2.3 m s^{-1}, T = 303.15 K, P = 1 atm.

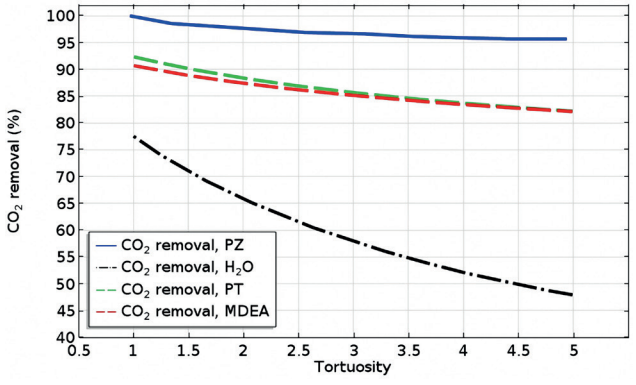

Fig. 11 The influence of membrane tortuosity on CO_2 removal using potassium threonate (PT), piperazine (PZ), pure water (H_2O) and methyldiethanolamine (MDEA) liquid absorbents.
Feed gas = 20/80 CO_2/CH_4, r_1 = 0.325 mm, r_2 = 0.5 mm, r_3 = 0.845 mm, $C_{CO2,0}$ = 0.075 mol m^{-3}, $C_{absorbents}$ = 1000 mol m^{-3}, V_g = 0.07 m s^{-1}, V_l = 2.3 m s^{-1}, T = 303.15 K, P = 1 atm.

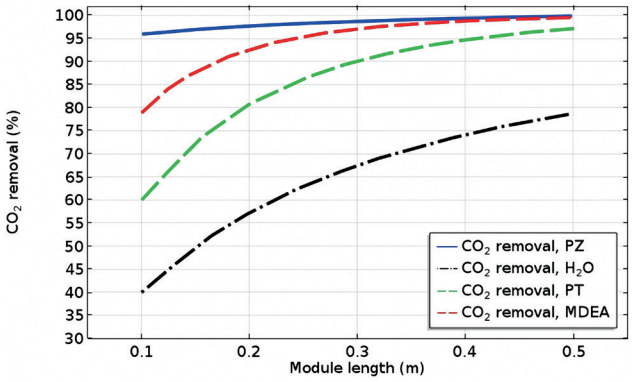

Fig. 12 The influence of module length on CO_2 removal using potassium threonate (PT), piperazine (PZ), pure water (H_2O) and methyldiethanolamine (MDEA) liquid absorbents.
Feed gas = 20/80 CO_2/CH_4, r_1 = 0.325 mm, r_2 = 0.5 mm, r_3 = 0.845 mm, $C_{CO2,0}$ = 0.075 mol m^{-3}, $C_{absorbents}$ = 1000 mol m^{-3}, V_g = 0.07 m s^{-1}, V_l = 2.3 m s^{-1}, T = 303.15 K, P = 1 atm.

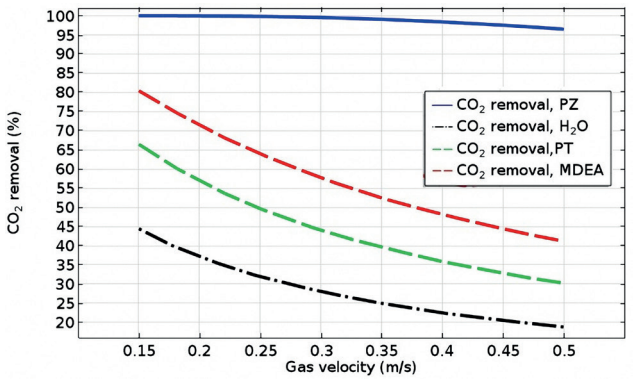

Fig. 13 The influence of gas velocity on CO_2 removal using potassium threonate (PT), piperazine (PZ), pure water (H_2O) and methyldiethanolamine (MDEA) liquid absorbents.
Feed gas = 20/80 CO_2/CH_4, r_1 = 0.325 mm, r_2 = 0.5 mm, r_3 = 0.845 mm, $C_{CO2,0}$ = 0.075 mol m^{-3}, $C_{absorbents}$ = 1000 mol m^{-3}, V_g = 0.07 m s^{-1}, V_l = 2.3 m s^{-1}, T = 303.15 K, P = 1 atm.

Fig. 12, while using PZ absorbent, the sequestration percentage of CO_2 from CO_2/CH_4 gaseous mixture improves from around 96 to 100 % when the module length increases from 0.1 to 0.5 m. Also using PT, H_2O and MDEA absorbing agents causes a substantial linear increment in the sequestration percentage of CO_2 from 60 to almost 97 %, from 40 to almost 78 % and from 79 to 99 %, respectively when the module length increases from 0.1 to 0.5 m.

4.7 The Effect of Gas Velocity on CO_2 Removal

Fig. 13 depicts the removal efficiency of CO_2 in a wide range of gas velocities applying PT, PZ, H_2O and MDEA liquid absorbents. As expected, increment of gas velocity results in a substantial decrease in the residence time in the hollow fiber membrane module. Even in the low velocity of gas, decrease in the sequestration percentage of CO_2 is completely apparent. As can be seen from the Fig. 13, by increasing the velocity of gas from 0.15 to 0.5 m s^{-1}, the removal percentage of CO_2 decreases drammatically from about 100 to nearly 96 % while using PZ absorbent solvent. Also Fig. 13 indicates that the increment of the velocity of gas from 0.15 m s^{-1} to 0.5 m s^{-1} resultes in a considerable decrease in the sequestration percentage of CO_2 from about 66 to nearly 30 %, from 15 to nearly 20 % and from 80 to 40 % while using PT, H_2O and MDEA, respectively.

5 Conclusion

In this investigational study a dynamic modeling and two dimensional comprehensive simulation is presented in order to assess the sequestration performance of CO_2 from CO_2/CH_4 gaseous stream in the hollow fiber membrane contactor. Four novel liquid absorbing agents including potassium threonate (PT), piperazine (PZ), pure water (H_2O) and methyldiethanolamine (MDEA) are applied with the aim of comparing their efficiency for CO_2 sequestration. The results of dynamic modeling and simulation indicated the superiority of PZ for removing CO_2 in comparison with PT, H_2O and MDEA liquid absorbents. Based on the abovementioned results, the amount of CO_2 removal from gaseous stream using PZ is approximately 100 % while the maximum CO_2 removal using MDEA, PT, and H_2O is about 96, 89 and 57 %, respectively. Comparison of modeling and two dimensional simulation results with the experimental data is implemented for investigating the accuracy of simulation and validating the simulation results. An average deviation of 3 % is seen between the results of two dimensional simulation and experimental data which confirms an excellent agreement. Increment of some operational parameters such as module length and porosity encourage the sequestration percentage of CO_2 from gaseous stream while some other parameters such as membrane tortuosity and gas velocity had negative effect on the removal of CO_2 from CO_2/CH_4 gaseous stream.

References

[1] Lin, S.-H., Chiang, P.-C., Hsieh, C.-F., Li, M.-H. Tung, K.-L. "Absorption of carbon dioxide by the absorbent composed of piperazine and 2-amino-2-methyl-1-propanol in PVDF membrane contactor", Journal of the Chinese Institute of Chemical Engineers, 39(1), pp. 13-21, 2008.
https://doi.org/10.1016/j.jcice.2007.11.010

[2] Pirouzfar, V., Hosseini, S. S., Omidkhah, M. R., Moghaddam, A. Z. "Modeling and optimization of gas transport characteristics of carbon molecular sieve membranes through statistical analysis", Polymer Engineering & Science, 54(1), pp. 147-157, 2014.
https://doi.org/10.1002/pen.23553

[3] Nakhjiri, A. T., Heydarinasab, A., Bakhtiari, O., Mohammadi, T. "Influence of non-wetting, partial wetting and complete wetting modes of operation on hydrogen sulfide removal utilizing monoethanolamine absorbent in hollow fiber membrane contactor", Sustainable Environment Research, 28(4), pp. 186-196, 2018.
https://doi.org/10.1016/j.serj.2018.02.003

[4] Zanganeh, K. E., Shafeen, A., Salvador, C. "CO_2 Capture and Development of an Advanced Pilot-Scale Cryogenic Separation and Compression Unit", Energy Procedia, 1(1), pp. 247-252, 2009.
https://doi.org/10.1016/j.egypro.2009.01.035

[5] Tuinier, M., van Sint Annaland, M., Kramer, G. J., Kuipers, J. A. M. "Cryogenic CO_2 capture using dynamically operated packed beds", Chemical Engineering Science, 65(1), pp. 114-119, 2010.
https://doi.org/10.1016/j.ces.2009.01.055

[6] Oexmann, J., Kather, A. "Post-combustion CO_2 capture in coal-fired power plants: Comparison of integrated chemical absorption processes with piperazine promoted potassium carbonate and MEA", Energy Procedia, 1(1), pp. 799-806, 2009.
https://doi.org/10.1016/j.egypro.2009.01.106

[7] Zhang, W., Ye, L., Jiang, J. "CO_2 capture with complex absorbent of ionic liquid, surfactant and water", Journal of Environmental Chemical Engineering, 3(1), pp. 227-232, 2015.
https://doi.org/10.1016/j.jece.2014.07.020

[8] Dindore, V. Y., Brilman, D. W. F., Feron, P. H. M., Versteeg, G. F. "CO_2 absorption at elevated pressures using a hollow fiber membrane contactor", Journal of Membrane Science, 235(1-2), pp. 99-109, 2004.
https://doi.org/10.1016/j.memsci.2003.12.029

[9] Qi, Z., Cussler, E. "Microporous hollow fibers for gas absorption: I. Mass transfer in the liquid", Journal of Membrane Science, 23(3), pp. 321-332, 1985.
https://doi.org/10.1016/S0376-7388(00)83149-X

[10] Blauwhoff, P. M. M., Versteeg, G. F., Van Swaaij, W. P. M. "A study on the reaction between CO_2 and alkanolamines in aqueous solutions", Chemical Engineering Science, 39(2), pp. 207-225, 1984.
https://doi.org/10.1016/0009-2509(84)80021-4

[11] Kim, Y.-S., Yang, S.-M. "Absorption of carbon dioxide through hollow fiber membranes using various aqueous absorbents", Separation and Purification Technology, 21(1-2), pp. 101-109, 2000.
https://doi.org/10.1016/S1383-5866(00)00195-7

[12] Ghadiri, M., Marjani, A., Shirazian, S. "Mathematical modeling and simulation of CO_2 stripping from monoethanolamine solution using nano porous membrane contactors", International Journal of Greenhouse Gas Control, 13, pp. 1-8, 2013.
https://doi.org/10.1016/j.ijggc.2012.11.030

[13] Faiz, R., Al-Marzouqi, M. "Mathematical modeling for the simultaneous absorption of CO_2 and H_2S using MEA in hollow fiber membrane contactors", Journal of Membrane Science, 342(1-2), pp. 269-278, 2009.
https://doi.org/10.1016/j.memsci.2009.06.050

[14] Nakhjiri, A. T., Heydarinasab, A., Bakhtiari, O., Mohammadi, T. "The effect of membrane pores wettability on CO_2 removal from CO_2/CH_4 gaseous mixture using NaOH, MEA and TEA liquid absorbents in hollow fiber membrane contactor", Chinese Journal of Chemical Engineering, 26(9), pp. 1845-1861, 2018.
https://doi.org/10.1016/j.cjche.2017.12.012

[15] Nakhjiri, A. T., Heydarinasab, A., Bakhtiari, O., Mohammadi, T. "Experimental investigation and mathematical modeling of CO_2 sequestration from CO_2/CH_4 gaseous mixture using MEA and TEA aqueous absorbents through polypropylene hollow fiber membrane contactor", Journal of Membrane Science, 565, pp. 1-13, 2018.
https://doi.org/10.1016/j.memsci.2018.07.095

[16] Atchariyawut, S., Jiraratananon, R., Wang, R. "Separation of CO_2 from CH_4 by using gas–liquid membrane contacting process", Journal of Membrane Science, 304(1-2), pp. 163-172, 2007.
https://doi.org/10.1016/j.memsci.2007.07.030

[17] Alavinasab, A., Kaghazchi, T., Ravanchi, M. T., Shabani, K. "Modeling of carbon dioxide absorption in a gas / liquid membrane contactor", Desalination and Water Treatment, 29(1-3), pp. 336-342, 2011.
https://doi.org/10.5004/dwt.2011.1204

[18] Shirazian, S., Moghadassi, A., Moradi, S. "Numerical simulation of mass transfer in gas–liquid hollow fiber membrane contactors for laminar flow conditions", Simulation Modelling Practice and Theory, 17(4), pp. 708-718, 2009.
https://doi.org/10.1016/j.simpat.2008.12.002

[19] Boucif, N., Favre, E., Roizard, D. "CO_2 capture in HFMM contactor with typical amine solutions: A numerical analysis", Chemical Engineering Science, 63(22), pp. 5375-5385, 2008.
https://doi.org/10.1016/j.ces.2008.07.015

[20] Mehdipour, M., Karami, M. R., Keshavarz, P., Ayatollahi, S. "Analysis of CO_2 Separation with Aqueous Potassium Carbonate Solution in a Hollow Fiber Membrane Contactor", Energy & Fuels, 27(4), pp. 2185-2193, 2013.
https://doi.org/10.1021/ef4000648

[21] Nakhjiri, A. T., Heydarinasab, A., Bakhtiari, O., Mohammadi, T. "Modeling and simulation of CO_2 separation from CO_2/CH_4 gaseous mixture using potassium glycinate, potassium argininate and sodium hydroxide liquid absorbents in the hollow fiber membrane contactor", Journal of Environmental Chemical Engineering, 6(1), pp. 1500-1511, 2018.
https://doi.org/10.1016/j.jece.2018.01.068

[22] Razavi, S. M. R., Shirazian, S., Nazemian, M. "Numerical simulation of CO_2 separation from gas mixtures in membrane modules: Effect of chemical absorbent", Arabian Journal of Chemistry, 9(1), pp. 62-71, 2016.
https://doi.org/10.1016/j.arabjc.2015.06.006

[23] Rezakazemi, M., Niazi, Z., Mirfendereski, M., Shirazian, S., Mohammadi, T., Pak, A. "CFD simulation of natural gas sweetening in a gas–liquid hollow-fiber membrane contactor", Chemical Engineering Journal, 168(3), pp. 1217-1226, 2011.
https://doi.org/10.1016/j.cej.2011.02.019

[24] Lohrasbi, S., Gorji-Bandpy, M., Ganji, D. D. "Thermal penetration depth enhancement in latent heat thermal energy storage system in the presence of heat pipe based on both charging and discharging processes", Energy Conversion and Management, 148, pp. 646-667, 2017.
https://doi.org/10.1016/j.enconman.2017.06.034

[25] Lohrasbi, S., Miry, S. Z., Gorji-Bandpy, M., Ganji, D. D. "Performance enhancement of finned heat pipe assisted latent heat thermal energy storage system in the presence of nano-enhanced H_2O as phase change material", International Journal of Hydrogen Energy, 42(10), pp. 6526-6546, 2017.
https://doi.org/10.1016/j.ijhydene.2017.01.045

[26] Eslami, S., Mousavi, S. M., Danesh, S., Banazadeh, H. "Modeling and simulation of CO_2 removal from power plant flue gas by PG solution in a hollow fiber membrane contactor", Advances in Engineering Software, 42(8), pp. 612-620, 2011.
https://doi.org/10.1016/j.advengsoft.2011.05.002

[27] Ho, W. S. W., Sirkar, K. K. "Membrane Handbook", 1st ed., Van Nostrand Reinhold, New York, USA 1992.

[28] Yang, M.-C., Cussler, E. L. "Designing hollow-fiber contactors", AIChE Journal, 32(11), pp. 1910-1916, 1986.
https://doi.org/10.1002/aic.690321117

[29] Gabelman, A., Hwang, S.-T. "Hollow fiber membrane contactors", Journal of Membrane Science, 159(1-2), pp. 61-106, 1999.
https://doi.org/10.1016/S0376-7388(99)00040-X

[30] Happel, J. "Viscous flow relative to arrays of cylinders", AIChE Journal, 5(2), pp. 174-177, 1959.
https://doi.org/10.1002/aic.690050211

[31] Srisurichan, S., Jiraratananon, R., Fane, A. G. "Mass transfer mechanisms and transport resistances in direct contact membrane distillation process", Journal of Membrane Science, 277(1-2), pp. 186-194, 2006.
https://doi.org/10.1016/j.memsci.2005.10.028

[32] Hwang, K.-S., Park, D.-W., Oh, K.-J., Kim, S.-S., Park, S.-W. "Chemical Absorption of Carbon Dioxide into Aqueous Solution of Potassium Threonate", Separation Science and Technology, 45(4), pp. 497-507, 2010.
https://doi.org/10.1080/01496390903529919

[33] Bishnoi, S., Rochelle, G. T. "Absorption of carbon dioxide into aqueous piperazine: reaction kinetics, mass transfer and solubility", Chemical Engineering Science, 55(22), pp. 5531-5543, 2000.
https://doi.org/10.1016/S0009-2509(00)00182-2

[34] Park, S.-W., Choi, B.-S., Lee, J.-W. "Chemical absorption of carbon dioxide with triethanolamine in non-aqueous solutions", Korean Journal of Chemical Engineering, 23(1), pp. 138-143, 2006.
https://doi.org/10.1007/BF02705705

[35] Wang, R., Li, D. F., Liang, D. T. "Modeling of CO_2 capture by three typical amine solutions in hollow fiber membrane contactors", Chemical Engineering and Processing: Process Intensification, 43(7), pp. 849-856, 2004.
https://doi.org/10.1016/S0255-2701(03)00105-3

[36] Sun, W.-C., Yong, C.-B., Li, M.-H. "Kinetics of the absorption of carbon dioxide into mixed aqueous solutions of 2-amino-2-methyl-l-propanol and piperazine", Chemical Engineering Science, 60(2), pp. 503-516, 2005.
https://doi.org/10.1016/j.ces.2004.08.012

[37] Portugal, A. F., Magalhães, F. D., Mendes, A. "Carbon dioxide absorption kinetics in potassium threonate", Chemical Engineering Science, 63(13), pp. 3493-3503, 2008.
https://doi.org/10.1016/j.ces.2008.04.017

[38] Hikita, H., Asai, S., Ishikawa, H., Honda, M. "The kinetics of reactions of carbon dioxide with monoethanolamine, diethanolamine and triethanolamine by a rapid mixing method", The Chemical Engineering Journal, 13(1), pp. 7-12, 1977.
https://doi.org/10.1016/0300-9467(77)80002-6

[39] Versteeg, G. F., van Swaaij, W. P. M. "Solubility and diffusivity of acid gases (carbon dioxide, nitrous oxide) in aqueous alkanolamine solutions", Journal of Chemical and Engineering Data, 33(1), pp. 29-34, 1988.
https://doi.org/10.1021/je00051a011

[40] Versteeg, G. F., van Swaaij, W. P. M. "On the kinetics between CO_2 and alkanolamines both in aqueous and non-aqueous solutions — I. Primary and secondary amines", Chemical Engineering Science, 43(3), pp. 573-585, 1988.
https://doi.org/10.1016/0009-2509(88)87017-9

[41] Kadiwala, S. "Absorption Rates of CO_2 in Aqueous and Non-Aqueous Amine Solutions and Solubility of CO_2 in Aqueous Piperazine Solution", University of Regina, Saskatchewan, Canada, 2008.

[42] Perrin, D. D. "Dissociation Constants of Organic Bases in Aqueous Solution", 4th ed., Butterworths, London, UK, 1972.

[43] Paul, S., Thomsen, K. "Kinetics of absorption of carbon dioxide into aqueous potassium salt of proline", International Journal of Greenhouse Gas Control, 8, pp. 169-179, 2012.
https://doi.org/10.1016/j.ijggc.2012.02.013

[44] Cussler, E. L. "Diffusion: Mass Transfer in Fluid Systems", 3rd ed., Cambridge University Press, Cambridge, UK, 2009.